Reduction of Simulation Times for High-Q Structures Using the Resonance Equation

Thomas Wesley Hall[1, 2, *], Prabhakar Bandaru[2], and Daniel Rees[1]

Abstract—Simulating steady state performance of high quality factor (Q) resonant RF structures is computationally difficult for structures with sizes on the order of more than a few wavelengths because of the long times (on the order of $\sim 0.1\,\mathrm{ms}$) required to achieve steady state in comparison with maximum time step that can be used in the simulation (typically, on the order of $\sim 1\,\mathrm{ps}$). This paper presents analytical and computational approaches that can be used to accelerate the simulation of the steady state performance of such structures. The basis of the proposed approach is the utilization of a larger amplitude signal at the beginning to achieve steady state earlier relative to the nominal input signal. The methodology for finding the necessary input signal is then discussed in detail, and the validity of the approach is evaluated.

1. INTRODUCTION

While the use of the finite-difference time-domain (FDTD) method for the analysis of radio-frequency components is well established [1–4], electrically large (more than a few wavelengths (λ) in one dimension) components require large simulation times that are computationally prohibitive. It is generally considered, based on the stability criteria of the finite difference formulas, that a minimum of 10 to 20 spatial grid points per the minimum simulated λ will be needed to ensure accurate results [1]. As the length scale to λ ratio increases, such requirements lead to a larger number of points that increases the calculation time.

This problem is greatly compounded for large structures at resonance. Steady state in such cases is reached in tens of thousands of periods for $Q >\sim 10,000$. The stability requirement for the time step (Δt) used in FDTD methods is [2]:

$$\Delta t \leq \frac{1}{c}\left[\left(\frac{1}{\Delta x}\right)^2 + \left(\frac{1}{\Delta y}\right)^2 + \left(\frac{1}{\Delta z}\right)^2\right]^{-1/2}, \tag{1}$$

where c is the speed of light, and Δx, Δy, and Δz are the smallest grid spacings in the three spatial dimensions. Knowing the grid spacings will be between $\lambda/10$ to $\lambda/20$, each period will require between 20 to 35 time steps to simulate. This means that hundreds of thousands to millions of time steps will be necessary to approach an acceptable steady state solution.

There have been several previous approaches to dealing with these long simulation times. For instance, it has been shown that relatively few time steps can be used to extrapolate the results to the steady state [2], and frequency domain methods [3] solve directly for the steady state solution. However, such methods neglect the details of how the fields change as the system reaches steady state. Such details are important in the analysis of any abnormalities that have been observed during real-world operation. Spectral methods, such as the pseudospectral time domain (PSTD) methodology, reduce the

* Corresponding author: Thomas Wesley Hall (twh@lanl.gov).
[1] Los Alamos National Laboratory, USA. [2] University of California, San Diego, USA.

mesh through calculating the spatial derivatives in Maxwells Equations using a Fourier transform based methodology [1, 4]. This reduces the mesh size to 2 grid points per λ based on the Nyquist sampling theorem. However, even these methods still require a large number of time-steps.

In this paper, we focus on the particular problem of a large (length of $\sim 10\lambda$) cavity resonator, as may be found in a linear accelerator. In addition to an optimization of the temporal and spatial cavity performance, specific phenomena which deteriorate/influence the cavity characteristics such as arcing [5] or multipactor [6, 7] are important in the design of these structures. Such phenomena often require calculation of the electromagnetic fields from both the input signal and the charged particle dynamics. In the previous studies, analysis of these phenomena during transient periods has not been well established in terms of the necessary spatial or time resolutions. It is then proposed to use an alternative methodology for such studies.
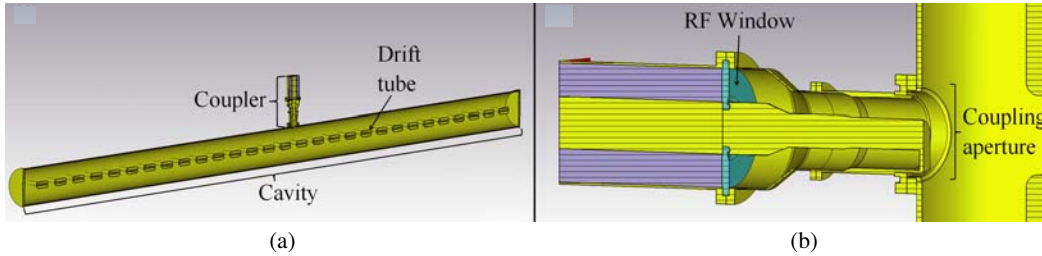

Figure 1. The accelerating cavity of a typical DTL. (a) shows the entire resonant cavity with drift tubes and the portion of the coupler nearest the cavity. (b) shows the coupler geometry.

The test case is based on the 201.25 MHz DTL at the Los Alamos Neutron Science Center (LANSCE). An example of such a cavity is shown in Fig. 1. Such structures utilize standing electromagnetic (EM) waves to accelerate charged particles across the resonant cavity. These accelerating fields are established by coupling the cavity to the power source via a waveguide or transmission line. Outside of the cavity, only the portion of the coaxial transmission line nearest the resonant cavity needs to be considered since this will most accurately simulate the cavity response to the input. In order to prevent deceleration as the fields switch polarity, drift tubes are added along the beamline. Consequently, there is a high degree of complexity in the designed geometry of such structures, which are often on the order of ~ 10 m long and ~ 1 m in diameter.

In order for the DTL to reach steady state, the cavity must be typically driven by an input signal for a time of ~ 0.1 ms. This long fill time is due to a number of factors, such as losses in the walls, the small percent of incident energy entering the cavity from the coupler, time for the summation of transient reflections to reach steady state, etc. Considering that the operation frequency is 201.25 MHz, the FDTD method for solving for the EM fields will require a time step on the order of 1–10 ps, as implied by (1). The large size of these structures (of $> 10\lambda$) and the high geometric complexity also means that there will be a large number (up to a few million) of points in the FDTD grid. Performing such simulations in parallel through two Intel Xeon® E5-2650 v2 2.6 GHz processors, takes a week or two to achieve results corresponding to steady state. It is then desirable to develop a technique that reduces the simulation times.

The principle of our methodology utilizes a signal that is significantly larger than the nominal signal to reach the steady state conditions more quickly. The nominal signal, henceforth referred to as the long fill, is a constant amplitude, sinusoidal signal that is used in the practical operation of the DTL. For this work, the amplitude of the long fill was set to the nominal value of $1 W^{1/2}$. The unit of $W^{1/2}$ comes from the interpretation of the input signal by our FDTD solver, as discussed in the next section. By increasing the amplitude of the long fill signal (by an amount calculated according to the next section) until some time t_1 and then linearly decreasing the amplitude to that of the long fill, a quick fill excitation is created. The quick fill consists of three regions: 1) Constant amplitude of P_0 from time 0 to t_1, 2) Linearly decreasing amplitude from P_0 to the nominal amplitude of 1 from times t_1 to t_2, and 3) Constant amplitude of 1 from time t_2 until the specified end time. This quick fill signal
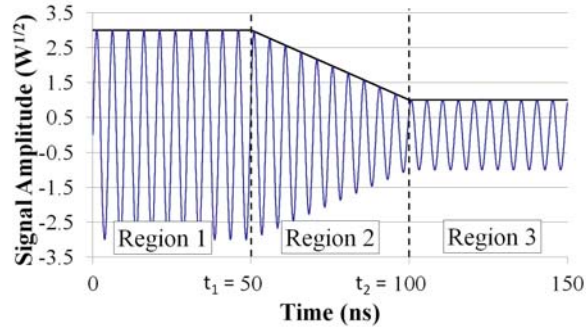
Figure 2. Example of input power signal with the three distinct regions labeled. Region 1 has a high constant amplitude, Region 2 decreases this amplitude in a linear manner to the nominal values held in Region 3. Region 3 is representative of steady state. This signal has a frequency of 201.25 MHz, but with t_1 and t_2 set to much lower values so the sinusoidal nature is apparent.

should provide the same steady state EM fields as the long fill. Fig. 2 shows an example of the quick fill signal with these regions labeled. The selection of times t_1 and t_2 should be an order of magnitude less than the fill time ($\sim 100\,\mu$s for a DTL), but still in the range of hundreds of periods, to ensure that any transient artifacts will be negligible.

2. GENERAL PROCEDURE

To validate the methodology of our approach and for comparison with the traditional methodologies, CST Microwave Studio was used. The formulation of the input signal requires knowledge of the resonant frequency of the mode to be analyzed, which was found by applying the FDTD solver to the specified frequency range of 200–350 MHz [8].

Our model incorporates one input/output port as shown in Fig. 3, so the resonant frequencies (f_0) can be readily calculated from the peaks in the ratio of the output to the input at each frequency (S-parameter). Once the f_0 is established, the input signal needs to be determined. In order to reach steady state with the long fill input, the signal must be run for a sufficiently long time. This time is the fill time and is on the order of $\sim 100\,\mu$s for the DTL.
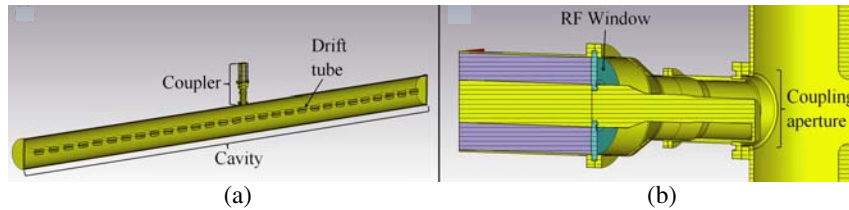

Figure 3. The two perfect electrical conductor (PEC) cases used in verification of the proposed methodology. (a) shows the geometry used in cases A and B, while the geometry of case C is shown in (b). All cases used the radius of the DTL cavity at LANSCE. Cases A and B used a height that is approximately 1 λ, and the length of case C was selected to accommodate four drift tubes of 0.352 m in length with a center-to-center distance of 0.559 m between them. The rectangle at the top of the coupler is the only input/output port in the system.

The determination of the input amplitudes for the quick-fill case requires an analysis of the response of the cavity to an input signal. This response can be found by considering the following relation for the vector potential $\vec{A}(\vec{r}, t)$ of the field inside the cavity [9]:

$$\nabla^2 \vec{A}(\vec{r}, t) - \frac{1}{c^2}\frac{\partial^2 \vec{A}(\vec{r}, t)}{\partial t^2} = -\mu \vec{J}_d r(\vec{r}, t) \tag{2}$$

where $\vec{J}_{dr}$ is the current density imposed by the input signal, and c and μ are the speed of light and magnetic permeability of the volume within the cavity. Further,

$$\vec{A}(\vec{r}, t) = \sum q_{mode}(t) \vec{A}_{mode}(\vec{r}) \tag{3}$$

where q_{mode} is the time dependent portion of the particular mode, and $\vec{A}_{mode}$ is the spatially dependent portion.

The driving current density can be separated in time and space $\vec{J}_{dr}(\vec{r}, t) = J_{dr}(t)\vec{J}(\vec{r})$, because while $\vec{J}(\vec{r})$ is dependent upon the coupler geometry, $J_{dr}(t)$ would be dependent upon the defined excitation signal. J_{dr} is considered to be directly proportional to the quick fill input P_{in}, so that $\vec{J}_{dr}(\vec{r}, t) = \chi P_{in}(t)\vec{J}(\vec{r})$, where χ is a constant with units of $W^{-1/2}$, the signal P_{in} has units of $W^{1/2}$, and both $\vec{J}_{dr}$ and $\vec{J}$ have the standard unit of A/m^2. These units arise from how CST interprets input signals at a port with an impedance of Z_0, such that the voltage between the inner and outer conductor and the current through the inner conductor are $V = P_{in}\sqrt{Z_0}$ and $I = P_{in}/\sqrt{Z_0}$ respectively (the units of I, V, and Z_0 are A, V, and Ω) respectively). Consequently,

$$\frac{\partial^2 q_{mode}}{\partial t^2} + 2\alpha \frac{\partial q_{mode}}{\partial t} + \omega_{mode}^2 q_{mode} = K P_{in}(t) \tag{4}$$

$$K = \chi \frac{\iiint_V \vec{J}(\vec{r}) \cdot \vec{A}_{mode}(\vec{r}) \, dV}{\varepsilon \iiint_V \vec{A}_{mode}^2 \, dV}. \tag{5}$$

The complete derivation of (4) can be found in the appendix. Estimation of α can be done by using the full-width, half-max (Δf) of the S-parameter peak of the mode being analyzed through:

$$\alpha = \frac{\omega_0}{2Q}, Q = \frac{f_0}{\Delta f} \Rightarrow \alpha = \pi \Delta f. \tag{6}$$

The general solution to (4) for a signal of linearly varying amplitude $K P_{in} = (m_i t + p_{0,i}) \sin(\omega t)$ is

$$q_{mode,i}(t) = (a_i \cos(\gamma t) + b_i \sin(\gamma t))e^{-\alpha t} + (c_{1,i}t + c_{2,i})\cos(\omega t) + (c_{3,i}t + c_{4,i})\sin(\omega t), \tag{7}$$

$$\gamma = \sqrt{\omega_{mode}^2 - \alpha^2} \tag{8}$$

The subscript i in (7) indicates which of the regions (corresponding to Fig. 2) the variables correspond to. The calculation of the coefficients a_i, b_i, and c_i is discussed in the appendix. Once a_i, b_i, and c_i have been determined for $i = 1, 2, 3$, the full response (q_{mode}) of the cavity to a given input signal ($K P_{in}$) is known.

The input $K P_{in}$ depends on three unknown parameters: t_1, t_2, and P_0. The values for t_1 and t_2 must be high enough that any transient artifacts from the EM fields propagating and reflecting off cavity surfaces will be negligible. However, since t_2 is the target time after which the system is at steady state, t_2 should also be significantly lower than the time required for the long fill to reach steady state. Beyond these two requirements, selection of t_1 and t_2 is arbitrary.

Once t_1 and t_2 have been selected, P_0 is found by applying different values of P_0 until the amplitude of q_{mode} is not changing by more than a defined tolerance of 10^{-8} (unitless) (see appendix) during the target steady state region. Two initial guesses for P_0 are made, then subsequent guesses are found by using the secant method [10]. The values used in the secant method are P_0 and the average change of the amplitude across the steady state region.

Once $K P_{in}$ is determined, the response of the system may now be evaluated. The validity of our approach was tested through a few test cases, which will be discussed next.

3. RESULTS AND DISCUSSION

Three test cases, incorporating the coupler and resonant cavity geometry found in the DTL, were used to validate the methodology of quick filling of the cavity through the use of a higher amplitude signal.

The exact dimensions of the coupler, the coupling aperture, and the cavity radius were kept for the simulations, but to decrease the simulation time, the cavity height was changed as shown in Fig. 3.

The first case was (A) a cylindrical cavity made of a perfect electric conductor (PEC) with no drift tubes. This geometry is shown in the top portion of Fig. 3. At steady state, the input and output signals will have the same amplitude as each other. The loss that contributes to α is the power emitting back from the cavity through the aperture into the coupler.

The next test case (B) corresponded to a copper (non PEC) cavity with the same geometry as case A. A higher α would be expected in this case due to the Ohmic resistance introduced in the cavity walls.

The last case (C) was a cavity with drift tubes added. PEC was selected as the cavity and drift tube material to remove the added complexity of Ohmic losses. This case was used to verify the overall validity of the approach with increased geometric complexity.

3.1. Cylindrical PEC Cavity

This test case was quick to simulate, and can also be modeled analytically, as discussed in the appendix. The specific geometry is found in Fig. 3. The radius corresponds to the cavity dimensions of the accelerator at LANSCE, and the height is about 1λ ($\sim 4.969\,\mathrm{m}$ for $201.25\,\mathrm{MHz}$). The frequency and α for this modified cavity were calculated from the S-parameter (only one value is necessary for the one port system) displayed in Fig. 4. These clearly show that the calculated resonant frequencies do in fact match the theoretical values obtained from the solution of Helmholtz Equation for a cylindrical cavity. The peak at $260.32\,\mathrm{MHz}$ was selected to be used for the demonstration of the quick-fill approach due to its correspondence to the fundamental TM_{010} mode. This varies from $f_0 = 201.25\,\mathrm{MHz}$ for the DTL at LANSCE due to the changed geometry of the cavity.
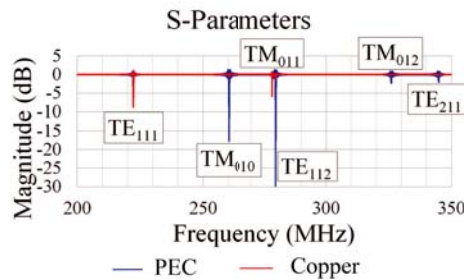

Figure 4. S-parameter of cases A and B. The peaks closely match in frequency to each other and the theoretical values of the labeled modes. Losses in the walls of the copper cavity change the relative strength of these modes from the PEC cavity, resulting in the difference in peak depths.

The values for the α, P_{in} and f_0 for this case and the other two cases are indicated in Table 1. The robustness of the quick filling method can be displayed by using a variety of times for t_1 and t_2. The value of t_2 was selected to be an order of magnitude less than the time required for the long fill to reach steady state ($\sim 1/\alpha$). This allows the system to reach steady state more quickly while still allowing any possible transient artifacts from interfering with the results.

The long fill case was also run until steady was reached at around $10{,}500\,\mathrm{ns}$ and compared to the simulations from the quick filling case. Fig. 5 shows the input/output (I/O) signals from the long fill and quick fill cases. The following criteria indicate the quick fill gives the same results as the long fill case.

The first criterion to consider is that the energy is constant over the steady state range. There is a variation of $0.035\,\mathrm{dB}$, or 0.2% (with respect to the maximum energy of the system) during the steady state. The second criterion is to ensure that the magnitude and phase of the output relative to the input is also matched between the long fill and quick fill cases. Because there are no Ohmic losses in the cavity, the magnitude of the output should be equal to the magnitude of the input at steady state ($1\,W^{1/2}$). The long fill and quick fill both showed this result.
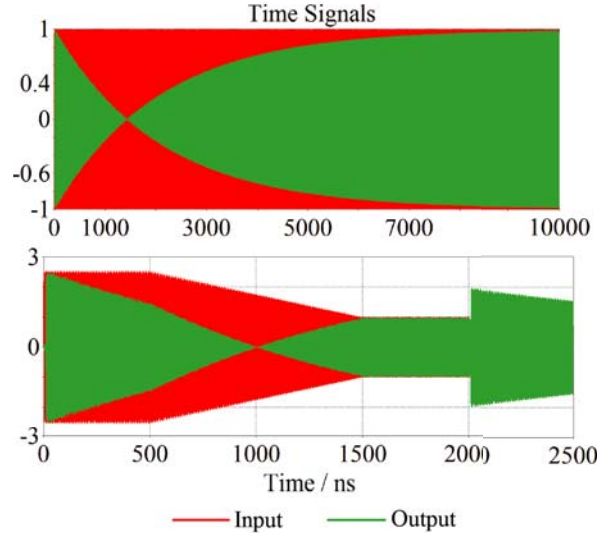
Figure 5. Input and output signals for the long fill (top) and quick fill (bottom) cases for the short PEC cavity. Both cases exhibit an initial decrease in output followed by an increase in output. The quick fill is able to achieve the same steady state output in 1,500 ns as opposed to 10,000 ns for the long fill. The input on the bottom portion is of the same shape as the signal in Fig. 2.
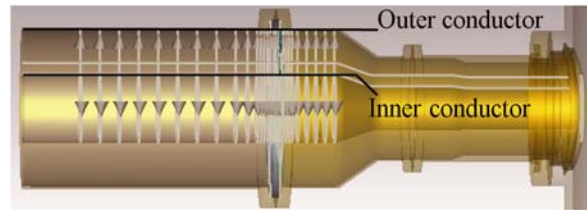

Figure 6. Voltage and current monitor locations along the coupler. The cavity is toward the right, with the monitors represented as grey arrows. The voltage monitors run from the inner to outer conductors, and the current monitors run in loops around the inner conductor.

The third criterion relates to the electric and magnetic field distributions within the coupler. For these simulations, voltage (V) and current (I) monitors were defined as shown in Fig. 6 The V will relate to the electric field distribution in the coupler, and I to the magnetic fields. Fig. 7 shows the respective distributions for both the long fill and quick fill cases. It is evident that the quick fill did successfully reach steady state because the profiles from the long and quick fill cases in Fig. 7 overlay exactly after 10 μs and 1.5 μs respectively.

3.2. Cylindrical Copper Cavity

This case was used to demonstrate that the quick-filling method is capable of filling a cavity made of lossy material. The values of α can be found in Table 1, and Fig. 4 illustrates that the S-parameter peaks for the copper cavity case were approximately the same in frequency but with different intensities. Because the strongest peak is now the TE_{111} mode at 222.855 MHz, this mode is analyzed in addition to the peak at 260.322 MHz corresponding to the TM_{010} mode.

Figure 7 shows the voltage and current profiles for the TM_{010} mode in both the PEC and the copper cavities. The profiles for the PEC cavity show excellent agreement between all long fill and quick fill simulations, as do all the profiles for the copper cavity. There are noticeable differences between the PEC and copper current profiles. This difference can be attributed to 1) a change in the time step used for the simulations, and 2) the change in the fields emitted from the cavity due to changes in the

Table 1. Parameters for various test cases of quick filling signals. An asterisk (*) indicates that the value for α was found using a least squares fit (11) of decay energy.

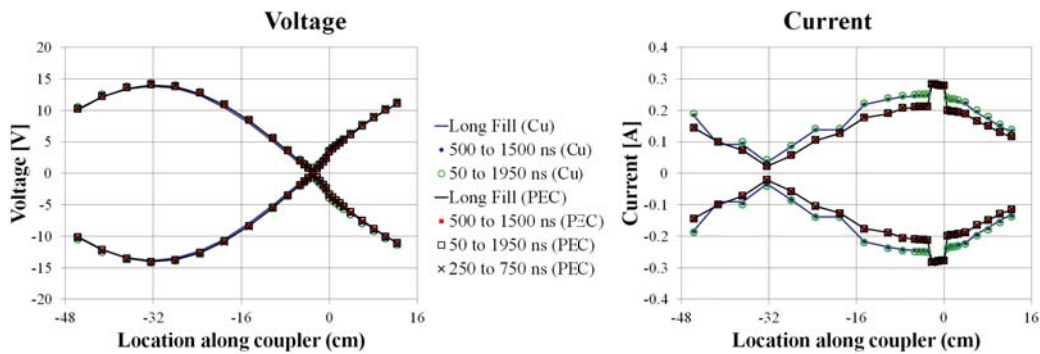| Case	f_0 (MHz)	$\alpha(10^{-5}$ ns$^{-1})$	$P_0(W^{1/2})$	t_1 (ns)	t_2 (ns)
A(i)	260.322	49.11	2.44	50	1,950
A(ii)	260.322	49.11	4.55	250	750
A(iii)	260.322	49.11	2.54	500	1,500
B(i)	260.322	49.70*	5.86	500	1,500
B(ii)	222.855	15.32	7.00	500	1,500
C(i)	215.489	2.24	9.41	2,500	7,500
C(ii)	215.489	1.02*	20.14	2,500	7,500

Figure 7. Voltage and current profiles in the steady state for the long fill and quick fill cases for the TM_{010} mode in the short PEC and copper cavities. The voltage profiles have good agreement between all cases. The current profiles show slightly higher values for the copper cavity.
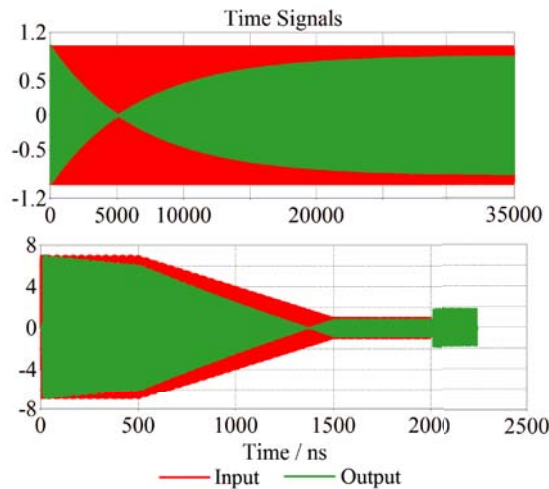
Figure 8. I/O signals for the long fill (top) and quick fill (bottom) cases of the TE_{111} mode in the copper cavity. The quick fill again reached steady state much more quickly than the long fill (1,500 ns vs. 35,000 ns).

boundary conditions introduced by the non-PEC material. An abrupt change can also be seen in the profiles near 0 in. This is the location of an RF window that has a relative electric permittivity of $\varepsilon = 2.53$. The change in the dielectric constant will directly affect the magnetic fields (analogous to the current profile).

The TE_{111} mode comparison between the long fill and quick fill inputs shows that the voltage and current profiles have excellent agreement between the long and quick fill cases. Fig. 8 shows the I/O waveforms for the two inputs and indicates that the output strength (indicated in green on the plot) is of equal magnitude ($\approx 0.96\,W^{1/2}$) for both the long fill and quick fill input waveforms. For the TE_{111} mode, steady state was reached in $35\,\mu s$ for the long fill case and in $1.5\,\mu s$ for the quick fill case. Furthermore, the field energy of the system validates that the system did in fact reach steady state as the difference between the maximum and minimum energies over the target steady state region (relative to the maximum) is only $0.04\,dB$, or 0.917%.

3.3. Truncated PEC Cavity with Drift Tubes

The last case considered was that of a cavity with drift tubes as shown in Fig. 3. The coupler offset was selected to accurately model an actual DTL at LANSCE, and the height was selected to accommodate four drift tubes, representing a small segment of the DTL at LANSCE. This geometry results in resonant frequencies that are slightly lower than with the previous two cases, as indicated in Table 1. Fig. 3 shows this geometry. Because the TM_{010} peak was much weaker for the copper case (see Fig. 4), the material for the cavity was selected to be PEC in order to ensure the S-parameters have a strong peak corresponding to this mode. PEC also implies that the output will be of equal magnitude to the input at steady state, giving us a way to check the validity of the approach without running the long fill, which would require $> 400\,\mu s$ to reach steady state.

The simulations did not result in the expected results that were observed for the previous cases. The amplitude of the output signal was about 10% that of the input, indicating that either α or ω_0 must have been erroneously calculated if the quick fill method is to be valid for increased geometric complexity. These were calculated from the S-parameter, which is itself calculated by applying a Fourier transform to the time dependent I/O signals [8]. As the S-parameter calculations run, the energy, and thus the emitted power, of the modes that have been excited by the input signal decrease, leading to the S-parameter peaks changing in height but not frequency. This means that α is likely to be miscalculated if the S-parameter calculations have not been run for a sufficient time. There is no method to predict the time for which the S-parameter calculations should be run, but this case ran for $50\,\mu s$ without producing reliable information to calculate α.

In order to accurately calculate α, a new method was considered. By using an input signal at the resonant frequency for a short time to partially fill the cavity, then bringing the input to zero, α can be calculated from the emitted output after the input has been brought to zero. The length of time that the cavity is filled should be sufficiently long enough such that the majority of the field energy is in the cavity and not the coupler. Finding t_{fill} (not to be confused with the quick filling parameters t_1 and t_2) can be difficult since α will still be unknown, but for this case we knew that it would have to be $\sim 1\,\mu s$ since the attempted quick fill of this cavity also required a time scale on the order of $\sim 1\,\mu s$ to achieve a partial fill. This quick fill information was not used to find α, however, because a standard procedure for calculating α needed to be tested. To calculate α, we used the definition of Q:

$$Q = 2\pi \frac{Energy\ stored\ in\ cavity}{Energy\ lost\ per\ cycle} = -\pi f_0 \frac{W}{\frac{\partial W}{\partial t}}. \tag{9}$$

The value of α can be found to be:

$$\alpha = \frac{\omega}{2Q} = -\frac{1}{W}\frac{\partial W}{\partial t}. \tag{10}$$

By solving this equation,

$$W(t) = Ce^{-\alpha t}, \tag{11}$$

where C is a coefficient that arises from the solution of (10). C is the field energy immediately after the input has been brought to zero, so its value will depend on t_{fill} and is not important to know for the quick fill. (11) is of a form that allows a least squares fit to be obtained for the decaying energy of a partially filled cavity. Fig. 9 shows the partial fill I/O signals and the energy. Using this new value of
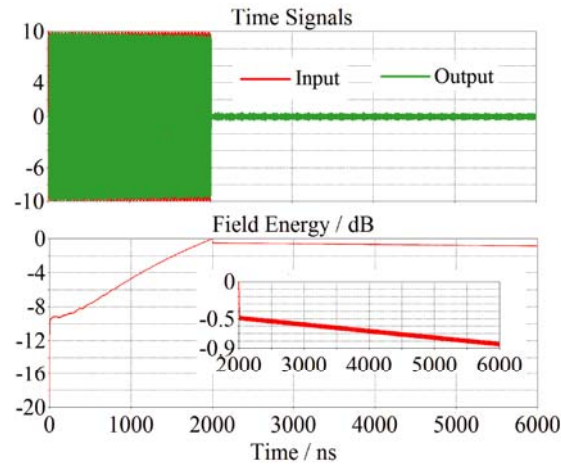
Figure 9. I/O signals (top) and relative field energy (bottom, in dB) of the partial fill used to calculate the attenuation coefficient. The inset plot of energy vs. time shows the data that is used to fit the parameters α and C in (11).
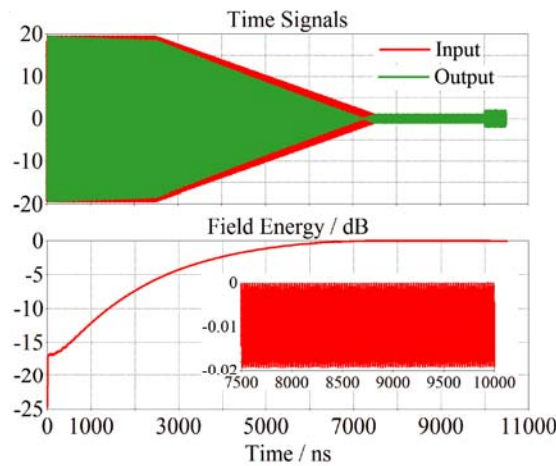

Figure 10. I/O signals (top) and relative field energy (bottom) of the quick fill for the PEC cavity with tubes using α calculated from the decay energy. The field energy varies by 0.02 dB from the maximum during the steady state period between 7,500 ns and 10,000 ns.

α (Case $C(ii)$ in Table 1), the value of P_0 was recalculated, and the simulation was run again with the new input signal. This run showed the results that were expected, as seen in Fig. 10. The output signal and energy both show that steady state was reached. In order to reach the same variation of 0.02 dB ($W/C = 0.0005$) with respect to the maximum energy during the steady state of the quick filling signal, the long fill signal would have to run for 0.527 ms as calculated from (11).

To ensure that this new approach for finding α is compatible with the previous two cases, α for those cases was re-calculated using the new method. A quick filling signal with times t_1 and t_2 set to 500 ns and 1,500 ns, respectively, was then calculated and applied based on these new values of α. (indicated in Table 2). The S-parameter also had to be re-calculated because of software updates that changed the resonant frequencies by $\sim 10^{-1}$–$10^{-2}\%$. The value of α calculated from the decay energy was not significantly different from α calculated from the S-parameter. The I/O signals of the quick fill calculated with both calculations of α show that there is excellent agreement for both values of α. This means that by carefully calculating α, the quick filling method gives accurate results.

Table 2. Recalculation of α and its effect on the simulation of steady state. For PEC this was performed at 260.1978 MHz (TM_{010}), and for copper at 222.296 MHz (TE_{111}).

Material	Calculation Method	$\alpha(10^{-5}\,\mathrm{ns}^{-1})$	Change in Energy over Steady State (dB)
PEC	S-parameter	48.83	-0.0201
PEC	Decay Energy	48.47	-0.0195
Copper	S-parameter	15.32	-0.0319
Copper	Decay Energy	14.94	-0.0214

4. SUMMARY

The use of a carefully estimated input signal can allow for the quick and efficient simulation of highly resonant, electrically large systems, resulting in simulation that run in ~ 2 hours as opposed to 2 days or more. This procedure was compared, through CST based simulations, to three test cases aimed at understanding better the performance/optimization of a 201.25 MHz DTL at LANSCE.

Three cases, i.e., (A) cylindrical PEC cavity, (B) a cylindrical copper cavity, and (C) a cylindrical PEC cavity with drift tubes, were successively considered, and used to verify the validity of the approach. The work also necessitated the implementation of a new method for calculating an attenuation factor, α. This factor provides information about the time frame for a resonant structure to reach steady state, so by applying an input signal for a short time (i.e., until the emitted signal from the cavity is detectable), this method allowed α to be found for more complex geometries.

While the quick fill method was developed for the specific case of a DTL, extensions can be made into similar problems requiring information about the transition to steady state. The voltage and current profiles along the coupler indicate that the EM fields are accurately simulated, meaning that this method can be employed to investigate phenomena that require knowledge of the EM fields as the steady state of the system is reached. In particular, these phenomena, such as arcing or multipactor, require calculations of physical attributes other than the EM fields that add to the computation time. Such problems can benefit from the decreased simulation times without affecting the accuracy of the results.

APPENDIX A.

A.1. Derivation and Application of the Resonance Equation

The derivation of (4) from (2,3) requires that the spatially dependent portion of the mode A_{mode} both satisfy the Helmholtz Equation and be orthogonal to other modes. Furthermore, using the definition of the Q-factor and its relation to an attenuation coefficient α, $Q = 2\pi \frac{Energy\ stored\ in\ cavity}{Energy\ lost\ per\ cycle} = \frac{\omega}{2\alpha}$, we obtain:

$$\frac{\partial^2 q_{mode}}{\partial t^2} + 2\alpha \frac{\partial q_{mode}}{\partial t} + \omega_{mode}^2 q_{mode} = \frac{\iiint_V \vec{J}(\vec{r}) \cdot \vec{A}_{mode}(\vec{r})\, dV}{\varepsilon \iiint_V \vec{A}_{mode}^2\, dV}. \tag{A1}$$

By applying the particular solution $q_{mode,particular,i}(t) = (c_{1,i}t + c_{2,i})\cos(\omega t) + (c_{3,i}t + c_{4,i})\sin(\omega t)$ to (4), the coefficients may then be determined through solving:

$$\begin{bmatrix} \omega_0^2 - \omega^2 & 0 & 2\alpha\omega & 0 \\ 2\alpha & \omega_0^2 - \omega^2 & 2\omega & 2\alpha\omega \\ -2\alpha\omega & 0 & \omega_0^2 - \omega^2 & 0 \\ -2\omega & -2\alpha\omega & 2\alpha & \omega_0^2 - \omega^2 \end{bmatrix} \begin{pmatrix} c_{1,i} \\ c_{2,i} \\ c_{3,i} \\ c_{4,i} \end{pmatrix} = \begin{pmatrix} 0 \\ 0 \\ m_i \\ P_{0,i} \end{pmatrix} \tag{A2}$$

After the coefficients for the particular solution have been found for each region, the coefficients a_i and b_i need to be determined. For region 1, this is done by setting both the value of q_{mode} in (7) and its time derivative equal to zero at time zero since all fields will be zero before the driving signal is started.

For the other regions, the continuity of the values and time derivatives of q_{mode} across regions is used to find the values of a and b by solving:

$$
\begin{bmatrix} \cos(\gamma t) & \sin(\gamma t) \\ -\alpha \cos(\gamma t) - \gamma \sin(\gamma t) & \gamma \cos(\gamma t) - \alpha \sin(\gamma t) \end{bmatrix} \begin{pmatrix} a_i \\ b_i \end{pmatrix} e^{-\alpha t} = \begin{pmatrix} q_{mode,i-1}(t) \\ q'_{mode,i-1}(t) \end{pmatrix}
$$
$$
- \left(\begin{matrix} [c_{1,i}t + c_{2,i}]\cos(\omega t) + [c_{3,i}t + c_{4,1}]\sin(\omega t) \\ [c_{3,i}\omega t + c_{1,i} + c_{4,i}\omega]\cos(\omega t) - [c_{1,i}\omega t + c_{2,i}\omega - c_{3,i}]\sin(\omega t) \end{matrix} \right), i = 2, 3 \tag{A3}
$$

For the nominal long fill signal, there is one region consisting of values $m = 0$ and $P_0 = 1$. This results in:

$$
q_{mode}(t) = \frac{1}{2\omega}\left(\frac{1}{\alpha}\cos(\gamma t) - \frac{1}{\gamma}\sin(\gamma t) \right) e^{-\alpha t} + \frac{1}{2\alpha\omega}\cos(\omega t) \tag{A4}
$$

It is obvious from (**??**) that the magnitude at steady state will be $\frac{1}{2\alpha\omega}$. For the quick fill signal, the values for m_i and $P_{0,i}$ are as follows:

$$
m = \begin{cases} 0 \\ \dfrac{1 - P_0}{t_2 - t_1} \\ 0 \end{cases}, \quad p_0 = \begin{cases} P_0 \\ \dfrac{t_2 P_0 - t_1}{t_2 - t_1} \\ 1 \end{cases} \quad \text{for} \quad \begin{matrix} t < t_1 \\ t_1 \leq t < t_2 \\ t \geq t_2 \end{matrix} \tag{A5}
$$

The value of P_0 is calculated for each set of geometries and times t_1 and t_2 by application of the secant method to the average change in the peak values of q_{mode} after time t_2. Two initial guesses are made for P_0, and then the coefficients a, b, and c are calculated for each region to get the values of q_{mode}. Then the peaks of q_{mode} after time t_2 are determined, and the time derivative of these peaks is calculated using finite difference formulas:

$$
y'_n = \begin{bmatrix} y_{n-1} & y_n & y_{n+1} \end{bmatrix} \begin{bmatrix} a \\ b \\ c \end{bmatrix}_n, \tag{A6}
$$

$$
\begin{bmatrix} \vec{h}_n^0 \\ \vec{h}_n \\ \dfrac{\vec{h}_n^2}{2} \end{bmatrix} \begin{bmatrix} a \\ b \\ c \end{bmatrix}_n = \begin{bmatrix} 0 \\ 1 \\ 0 \end{bmatrix}, \tag{A7}
$$

$$
\vec{h}_n = \begin{bmatrix} t_{n-1} & t_n & t_{n+1} \end{bmatrix}. \tag{A8}
$$

where y is a local peak value of q_{mode}. This is then used to determine the average of the time derivative of the peak values over steady state $\bar{y}$. Subsequent values of P_0 are calculated using:

$$
P_{0,n+1} = P_{0,n} - \bar{y}_n \frac{P_{0,n} - P_{0,n-1}}{\bar{y}_n - \bar{y}_{n-1}} \tag{A9}
$$

until $\bar{y}$ is sufficiently close to zero. Considering the maximum amplitude for steady state from (**??**), a tolerance of $< 10^{-8}$ to 10^{-12} will give accurate values of P_0 for a large range of structures.

A.2. Modal Analysis of the PEC Cavity

The analytic model for modes in cylindrical coordinates gives the overall wavenumber as:

$$
k^2 = \omega^2 \mu \varepsilon = k_\rho^2 + k_z^2 \tag{A10}
$$

where for TM modes:

$$
k_\rho^2 = \frac{\chi_{mn}}{r}, \; J_m(\chi_{mn}) = 0, \; k_z^2 = \frac{p\pi}{h} \tag{A11}
$$

and for TE modes:

$$k_\rho^2 = \frac{\chi'_{mn}}{r}, \ J'_m(\chi'_{mn}) = 0, \ k_z^2 = \frac{p\pi}{h} \tag{A12}$$

where χ_{mn} is the nth zero of the Bessel function of the order mJ_m (distinct from the χ in $\vec{J}_{dr}(\vec{r}, t) = \chi P_{in}(t)\vec{J}(\vec{r})$), χ'_{mn} is the nth zero of the derivative of the Bessel function of the order mJ'_m, r is the radius, and h is the height of the cylinder. Solution of these parameters is summarized in Table A1.

Table A1. Calculation of the theoretical frequencies of the simple PEC cavity.

Type	mn	χ_{mn} or χ'_{mn}	p	f (MHz)
TM	01	2.404826	0	260.30
TM	01	2.404826	1	278.26
TE	11	1.841184	1	222.24
TM	01	2.404826	2	326.27
TE	21	3.054237	1	344.91
TE	11	1.841184	1	280.02

REFERENCES

1. Liu, Q. H., "The PSTD algorithm: A time-domain method requiring only two cells per wavelength," *Microwave and Optical Technology Letters*, Vol. 15, No. 3, 158–165, 1997.
2. Shaw, A. K. and K. Naishadham, "Efficient ARMA modeling of FDTD time sequences for microwave resonant structures," *IEEE Trans. Microwave Theory Tech., Microwave Symposium Digest*, Vol. 1, 341–344, 1997.
3. Bondeson, A., T. Rylander, and P. Ingelström, *Computational Electromagnetics*, Springer, 2005.
4. Lee, T. W. and S. C. Hagness, "Pseudospectral time-domain methods for modeling optical wave propagation in second-order nonlinear materials," *Journal of the Optical Society of America B*, Vol. 21, No. 2, 2004.
5. Insepov, Z., J. Norem, et al., "Modeling RF breakdown arcs," arXiv:1003.1736, 2011.
6. Kravchuk, L. V., G. V. Romanov, and S. G. Tarasov, "Multipactoring code for 3D accelerating structures," arXiv:physics/0008015, 2000.
7. Cummings, K. A. and S. H. Risbud, "Dielectric materials for window applications," *Journal of Physics and Chemistry of Solids*, Vol. 61, No. 4, 2000.
8. CST Studio Suite, CST, www.sct.com.
9. Wangler, T. P., *RF Linear Accelerators*, Wiley-VCH, 2008.
10. Allen, M. B. and E. L. Isaacson, *Numerical Analysis for Applied Science*, Wiley, 2011.